

스프레이 특성에 가솔린 - 바이오 디젤 혼합 연료의 효과

삭다 통사이¹ · 임옥택^{2†}

¹울산대학교 기계자동차공학과 대학원, ²울산대학교 기계자동차공학부

The effects of Gasoline-Biodiesel Blended Fuels on Spray Characteristics

SAKDA THONGCHAI¹, OCKTAECK LIM^{2†}

¹Graduate of Mechanical and Automotive Engineering, University of Ulsan, Mugeo-dong, Nam-gu, Ulsan 680-749, Korea

²Department of Mechanical and Automotive Engineering, University of Ulsan, 102 Daehak-ro, Nam-gu, Ulsan 680-749, Korea

Abstract >> The current study has investigated the effects of biodiesel blended with gasoline on the spray characteristics in a Constant Volume Combustion Chamber (CVCC). With the concentration of 5, 10, 15 and 20% by volume, biodiesel was blended with commercial gasoline and performed on the macroscopic visualization test. Pure gasoline and biodiesel were also tested as the reference. The shadowgraph technique was conducted in the constant volume chamber. The spray images were recorded by a high speed video camera with frame speed 10,000 frame per second. Fuel injection was set at 800, 1000 and 1,350 bar with the simulated speed 1,500 and 2,000 rpm. The back pressure was controlled at 20 bar. The spray angle and penetration tip were measured and analyzed by using the image processing. At the high injection pressure, the spray penetration length with the simulated speed 1,500 rpm showed that B100 was lower than GB00-20 whereas the spray penetration length with the simulated speed 2,000 rpm exhibited that GB blends and B100 were insignificantly different. Due to biodiesel concentration, its effects on spray angles were observed throughout injection periods (T1, T2 and T3). At the simulated speed 1,500 rpm, the spray angle of GB blends and B100 presented the same pattern following injection timing. In addition, when the simulated speed increased to 2,000 rpm the different spray angle of all blends disappeared at main injection (T3).

Key words : Gasoline-Biodiesel Blended(가솔린 - 바이오 디젤 혼합), Spray Characteristics(스프레이 특성), Shadowgraph(그림자 그림)

Nomenclature

θ : spray cone angle

ATDC : after top dead center

B100 : neat biodiesel

BTDC : before top dead center

CAD : crank angle degree

CVCC : constant volume combustion chamber

GB00 : neat gasoline

GB05 : gasoline 95% + biodiesel 5%

GB10 : gasoline 90% + biodiesel 10%

GB15 : gasoline 85% + biodiesel 15%

GB20 : gasoline 80% + biodiesel 20%

GCI : gasoline compression ignition

HCCI : homogeneous charge compression ignition

L : spray penetration length

[†] Corresponding author : otlim@ulsan.ac.kr

Received : 2015.5.8 in revised form : 2015.6.24 Accepted : 2015.6.30

Copyright © 2015 KHNES

PFV : photron fastcam viewer
 RPM : revolution per minute
 T1 : pilot injection
 T2 : pre injection
 T3 : main injection

1. Introduction

The high demand of petroleum based fuel conjunction with the decreasing its resource has stimulated many researchers to investigate the new source of energies such as alternative fuels. Biodiesel has been successfully applied in many countries. However, the application has been limited in only the compression ignition engines. Therefore, it is interesting to use biodiesel in other types of engine, for instance, homogeneous charge compression ignition (HCCI) or gasoline compression ignition (GCI) engines¹⁾.

The spray characteristics, the product of fuel injections, have the significant effects on combustion and emissions of engines. Therefore, the spray behaviors should be carefully investigated. Many researches have studied the spray characteristics of biodiesel fuel. Szybist and Boehman²⁾ found that biodiesel could advance the fuel injection timing and shorten injection duration when compared with diesel. For spray pattern, longer penetration tip with narrower spray angle was presented for biodiesel injection³⁾. However, Allocca and et al could not find the difference of spray pattern between biodiesel and diesel⁴⁾.

Gasoline direct injection via diesel common rail injection system has been investigated recently⁵⁾. They

found that spray penetration between diesel and gasoline showed not clear differences but mass flow rate of gasoline was lower than diesel due to its lower density.

For gasoline blended with biodiesel, there are a few researches to study the spray characteristics when injecting with diesel common rail injection system. To understand the GB spray behaviors, the CVCC and one-hole injector were employed to investigate the spray length and cone angle. The effects of injection pressure and engine speed have been clarified. The spray characteristics were analyzed by image processing from Matlab.

2. Methodology

The spray characteristics were conducted in CVCC via shadowgraph technique with variety of blended biodiesel concentrations⁶⁾. The injection pressure was controlled by means of a diesel common rail system. The spray images were recorded by a high speed camera. Then, the image processing (Matlab) technique was employed to analyze the spray length and cone angle^{7,8)}.

2.1 Test fuel

Conventional gasoline from a retail station and neat biodiesel from an industrial were utilized in this study. The gasoline-biodiesel blends (GB) were mixed by percentage of volume. The concentrations of biodiesel were varied between 0 to 20% with 5% increment (GB00-GB20), where G stands for gasoline and B stands

Table 1 Physical properties of GB

| Properties | Unit | Test method | GB00 | GB05 | GB10 | GB15 | GB20 | B100 |
|---------------------|--------------------|---------------------|---------------------|-------|-------|-------|-------|-------|
| Kinematic Viscosity | mm ² /s | KS M ISO 3104:2008 | 0.735 ⁹⁾ | - | - | - | - | 4.229 |
| Density | kg/m ³ | KS M ISO 12185:2003 | 712.7 | 722.3 | 732.2 | 742.6 | 757.1 | 882.3 |

for biodiesel and the numeric value refers to the percentage by volume of biodiesel mixed with gasoline. Some of the physical properties of GB following Korean standard were exhibited in Table 1.

2.2 Spray visualization system

Fig. 1 exhibits the schematic diagram of the spray visualization system. The volume of CVCC is approximately 1,295 ml. It has six changeable ports such as quartz windows, injector and gas inlet and outlet port.

The common rail injection system consists of low pressure pump, common rail, one-hole injector, pressure controller, common rail solenoid injector peak & hold driver and multistage engine controller.

With knife edge technique, a high speed camera, Photron model SA3 was used to record the shadow spray pattern from light source through corrector lens. After recording at a speed of 10,000 frames/second, a thousand of spray images were transferred and saved in the personal computer via Photron FASTCAM Viewer (PFV) software.

2.3 Test condition

The blended fuels, GB00, GB05, GB10, GB15, and GB20 were injected into the CVCC with the simulated speed 1,500 and 2,000 rpm. Each of simulated speed has three injection timing including pilot injection (T1), pre-injection (T2) and main injection (T3) as shown in Table 2. The injection pressures were controlled at 800,

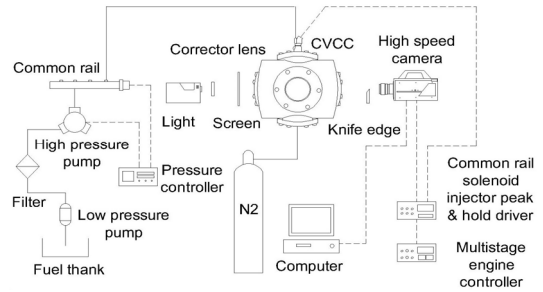


Fig. 1 The schematic diagram of the spray visualization system

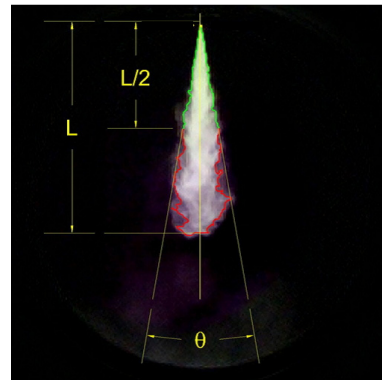


Fig. 2 The definition of the spray penetration length and the spray cone angle

1,000 and 1,350 bar. When the test fuel was injected into the CVCC, the common rail peak and hold driver triggered the high speed camera to record the image. The back pressure was set constantly at 20 bar. Each test condition was repeated 5 times.

The spray penetration length and the spray cone angle are defined in Fig. 2. The spray penetration length (L) is the distance from injector tip to the end of fuel spray. The spray cone angle (θ) is the angle which created by the

Table 2 The simulated speed

| 1,500 rpm | | 2,500 rpm | |
|------------------------|---------------|------------------------|---------------|
| Timing | Duration (ms) | Timing | Duration (ms) |
| Pilot: 10CAD BTDC (T1) | 300 | Pilot: 31CAD BTDC (T1) | 260 |
| Pre: 3CAD BTDC (T2) | 300 | Pre: 3CAD BTDC (T2) | 330 |
| Main: 6CAD ATDC (T3) | 700 | Main: 7CAD ATDC (T3) | 840 |

line covering the spray from the injector tip to the middle length of fuel spray.

3. Results and Discussion

The spray patterns of tested fuels with the simulated speed 1,500 rpm are fully developed after start of injection (SOI) at 3.3 ms as shown in Fig. 3(a). The results show that with the lower biodiesel concentration, the spray pattern is narrower and more uniform distribution.

The spray patterns of tested fuels with the simulated speed 2,000 rpm are fully developed at 5.4 ms as shown in the Fig. 3(b). They have the similar trend to the spray patterns at 1,500 rpm but the spray lengths are longer

because of their longer injection period (840 ms).

The injection timing and duration with the simulated speed 1,500 and 2,000 rpm and ambient temperature 25°C are shown Fig. 4 and 5 respectively. The spray images show the injection time in which the fuel is

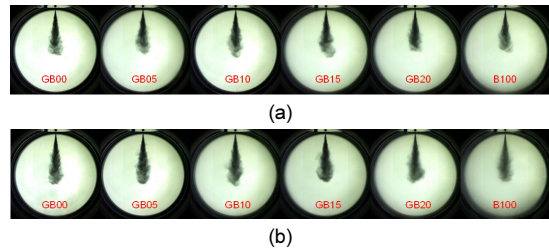


Fig. 3 The fully developed spray length and cone angle at injection pressure 1,350 bar with the simulated speed (a) 1,500 rpm and (b) 2,000 rpm

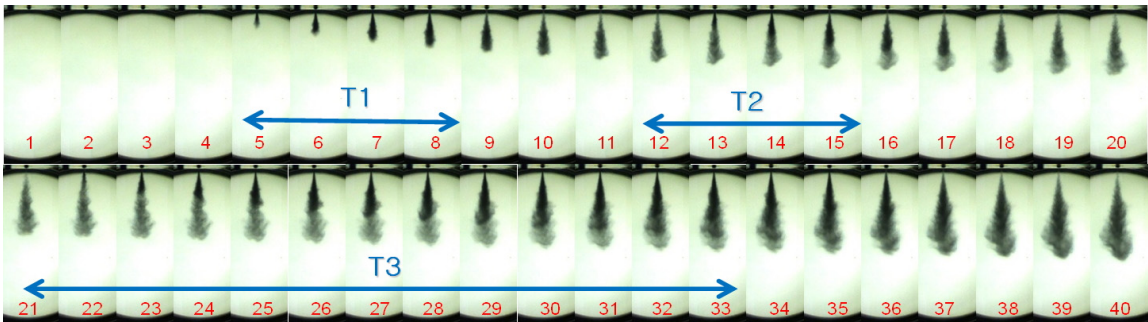


Fig. 4 Fuel injection times (x 0.1 ms) of 1,500 rpm at 25°C (GB05@1350 bar)

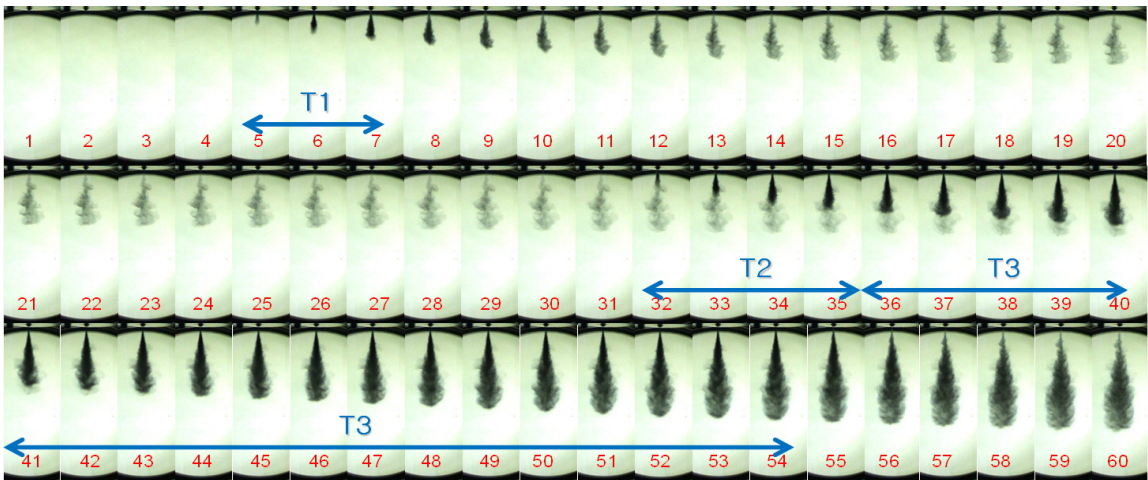


Fig. 5 Fuel injection times (x 0.1 ms) of 2,000 rpm at 25°C (GB05@1350 bar)

injected from the nozzle. At simulated speed 1,500 rpm, the images show that the injector are energized for T1 from 0.5 to 0.8 ms, T2 from 1.2 to 1.5 ms and T3 from 2.1 to 3.3 ms as well as the simulated speed 2,000 rpm, the injector are driven for T1 from 0.5 to 0.7 ms, T2 from 3.2 to 3.5 ms and T3 from 3.6 to 5.4 ms.

The spray penetration lengths and the spray cone angles are clearly specified by using the image processing. with the simulated speed 1,500 rpm and injection pressure 1,350 bar, GB00-20 and B100 show the similar patterns during T1, T2 and T3.

With the simulated speed 1,500 rpm, the spray penetration lengths of GB00-20 are in the vicinities due to the low concentration of biodiesel. When GB00-20 are compared with B100, their spray penetration length are slightly longer at the injection periods of T2 and T3 as shown in Fig. 6(a). At the simulated speed 2,000 rpm, there is no significant difference of the spray penetration

lengths between the blended fuels and B100 at all injection timing due to continuous injection period of T2 and T3 as shown in Fig. 6(b).

The spray cone angles at injection pressure 1,350 bar with the simulated speed 1,500 rpm are shown in Fig. 7(a) and (b). The results exhibit that the similar trends are observed for all tested fuels.

At the T1 injection period, the spray cone angles of all test fuels fluctuate and relatively broaden. According to Table 1, when the percentage of biodiesel is increased in the gasoline, the density of the blends increases due to the higher density of the biodiesel. The GB blends have lower density when comparing with the Korean standard ($815-835 \text{ kg/m}^3$)¹⁰. Thus, higher density results in larger fuel flow resistance which is the cause of higher viscosity. The kinematic velocity of neat biodiesel is higher than neat gasoline. Therefore, it may lead to inferior fuel injection¹¹. Meanwhile, GB00 at the injection periods of

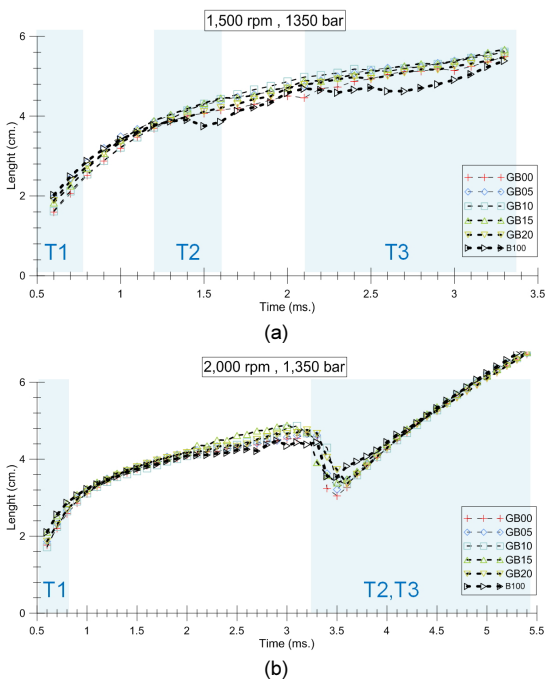


Fig. 6 The spray length at injection pressure 1,350 bar with the simulated speed (a) 1,500 rpm and (b) 2,000 rpm

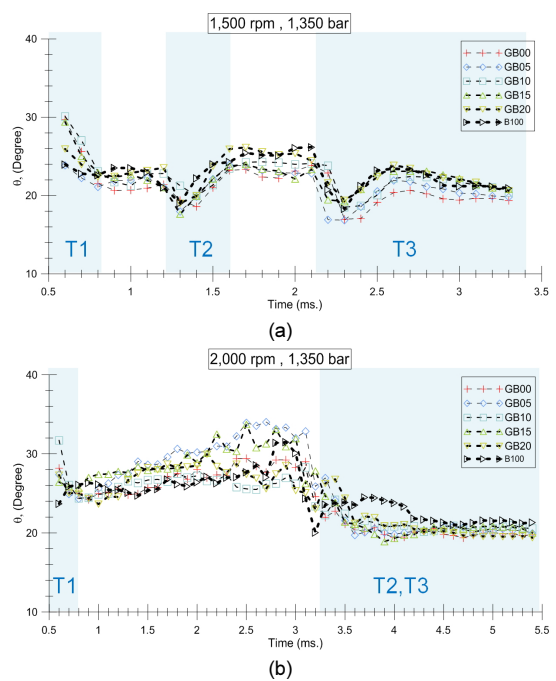


Fig. 7 The spray angle at injection pressure 1,350 bar with the simulated speed (a) 1,500 rpm and (b) 2,000 rpm

T2 and T3 shows the smallest spray cone angle due to its low density and viscosity value. Whereas, the B100 has the biggest spray cone angle which is similar to GB20. In addition, The cone angles of GB05-15 locate between GB00 and B100 values.

At the simulated speed 2,000 rpm and injection pressure 1,350 bar, the spray cone angles at the T1 injection period also fluctuate like the spray cone angles with the simulated speed 1,500 rpm. The spray cone angle of the GB00-20 at the injection periods of T2 and T3 are lower than B100 due to density and viscosity. Moreover, the spray cone angles of all tested fuel become narrow angle at the end of T3 injection period.

The spray penetration lengths and the spray cone angle of injection pressure 800 and 1,000 bar with the simulation speed 1,500 and 2,000 rpm are not shown here, because their results are similar to the results of injection pressure at 1,350 bar.

4. Conclusion

The results of spray penetration length and spray cone angle can be concluded as following:

- 1) GB00-20 and B100 at high injection pressure show the same spray penetration length and the spray cone angle patterns when the blended fuels are injected by diesel common rail injection system.
- 2) During the injection duration T3, the spray penetration length of B100 at 1,350 bar with simulation speed 1,500 rpm is lower than GB00-20. However, there is no significant difference of the spray penetration length between B100 and GB00-20 at 2,000 rpm and 1,350 bar.
- 3) For the spray cone angle, B100 is bigger than that of blended fuels.

Acknowledgement

This work was supported by the Energy Efficiency & Resources of the Korea Institute of Energy Technology Evaluation and Planning (KETEP) grant funded by the Korea government Ministry of Trade, Industry & Energy (MOTIE). (20122020100270), the Ministry of Education(MOE) and National Research Foundation of Korea (NRF) through the Human Resource Training Project for Regional Innovation and Basic Science Research Program through the National Research Foundation of Korea (NRF) funded by the Ministry of Education, Science and Technology (2012R1A1A1044855) and the development program of local science park funded by the Ulsan Metropolitan City and the Ministry of Education.

References

1. Internal Combustion Engine Fundamentals, John B. Heywood, International Edition 1998, McGRAW HILL, ISBN 0-07-100499-8.
2. J. P. Szybist, and A. L. Boehman, Behavior of a diesel injection system with biodiesel fuel. SAE Paper 2003-01-1039.
3. J. M. Desantes, R. Payri, F. J. Salvador, and J. Manln, Influence on diesel injection characteristics and behavior using biodiesel fuels. SAE Paper 2009-01-0851.
4. L. Allocca, E. Mancaruso, A. Montanaro, B. M. Vaglieco, and A. Vassallo, Renewable biodiesel/reference diesel fuel mixtures distribution in non-evaporating and evaporating conditions for diesel engines. SAE Paper 2009-24-0054.
5. R. Payri, A. Garcia, V. Domenech, R. Durrett, and A. P. Torres, Hydraulic behavior and spray characteristics of a common rail diesel injection system using gasoline fuel. SAE Paper 2012-01-0458.

6. Schlieren and shadowgraph Techniques, G. S. Settles, 1st edition 2001, Springer, ISBN 13 978-3-540-66155-9.
7. Digital Image Processing Using MATAB, Rafael C. Gonzalea, Richard E. Woods, Steven L. Eddins, Second Edtion 2009, Gatesmark Publishing, ISBN 978-0-9820854-0-0.
8. Image Processing Toolbox™, User's Guide R2014b, MatWorks Inc., 1993-2014, The MathWorks, Inc. 3 Apple Hill Drive, Natick, MA 01760-2098.
9. Yongming Bao, Qing Nian Chan, Sanghoon Kook, and Evatt Hawkes, "Spray Penetrations of Ethanol, Gasoline and Iso-Octane in an Optically Accessible Spark-Ignition Direct-Injection Engine", The University of New South Wales, SAE International, 2014-01-9079.
10. J. K. Kim, C. H. Jeon, E. S. Yim, and C. S. Chung, "Lubricity Characterization of Hydrogenated Biodiesel as an Alternative Diesel Fuel", Petroleum Technology R&D Center, Korea Institute of Petroleum Management, Journal of the KSTLE Vol. 28, No. 6, December 2012, pp. 321-327.
11. S. A. Shahirn, H. H. Masjuki, M. A. Kalam, A. Imran, I. M. Rizwanul Fattah, A. Sanjid, "Feasibility of diesel-biodiesel-ethanol/bioethanol blend as existing CI engine fuel: An assessment of properties, material compatibility, safety and combustion", Centre for Energy Sciences, Faculty of Engineering, University of Malaya, Renewable and Sustainable Energy Reviews, Vol. 32, 2014, pp. 379-395.